Applied Radiation and Isotopes 154 (2019) 108866

Contents lists available at ScienceDirect

Applied Radiation and Isotopes

journal homepage: www.elsevier.com/locate/apradiso

# Measurement of neutron induced $^{86}$Sr(n, 2n)$^{85}$Sr reaction cross sections at different neutron energies

Nidhi Shetty[a,**], Rajnikant Makwana[a,*], Mayur Mehta[a,b], S. Mukherjee[a], N.L. Singh[a], S.V. Suryanarayana[c], S. Parashari[a], R. Singh[a], H. Naik[d], S.C. Sharma[c], S. Ayyala[e], B. Soni[a], R. Chauhan[a]

[a] Department of Physics, Faculty of Science, The M. S. University of Baroda, 390002, India
[b] Institute for Plasma Research, Gandhinagar, 382428, India
[c] Nuclear Physics Division, Bhabha Atomic Research Centre, Trombay, Mumbai, 400085, India
[d] Radiochemistry Division, Bhabha Atomic Research Centre, Trombay, Mumbai, 400085, India
[e] G.B. Pant University of Agri. & Tech, Pantnagar, Uttarakhand, 263145, India

A B S T R A C T

The cross-sections for $^{86}$Sr (n, 2n)$^{85}$Sr reaction are measured at neutron energies 19.44 ± 1.02 MeV and 16.81 ± 0.85 MeV wherein there is scarcity of data. The standard neutron activation analysis technique and offline gamma ray spectroscopy have been employed for measurement and analysis of the data. The results are compared with experimental data available in EXFOR database, JEFF-3.3, JENDL-4.0, TENDL-2017 and ENDF/B-VIII.0 evaluated data. The theoretical prediction was incorporated using nuclear modular codes TALYS 1.8 and EMPIRE 3.2.2. A detailed comparative study of experimental results with the theoretical models and various major evaluations has been presented.

## 1. Introduction

Nuclear reaction cross-section data play a crucial role in the development of nuclear reactor technology. Neutrons covering a wide energy range are produced while a nuclear reactor is in operation. These neutrons tend to penetrate through various materials of the reactor which leads to a change in the physical properties and chemical composition of the materials present inside the reactor. Thus, it is imperative that nuclear reaction data be made available at all possible neutron energies for the development of the reactor technology (Koning and Blomgren, 2009; Dyakonov et al., 1994; Zsolnay et al., 2012). Strontium (Sr) is used in a superconducting magnet in fusion reactors (Soni et al., 2018). Sr-90 is useful as one of the high energy beta-emitters and also finds applications in space technology and oncology especially in cancer treatments. However, highly toxic Sr-90 is a by-product of nuclear reactors and is present in nuclear fallout. EXFOR (ExchangeFORmat) database library is the main worldwide repository of experimental data, which store all the measured nuclear data (EXFOR). However, it is essential that the existing available data be updated with better accuracy and new data be measured within energy range of thermal to 20 MeV. Also, accurate experimental data plays a vital role of validating various theoretical nuclear models. In the present work, the cross-sections of $^{86}$Sr (n, 2n)$^{85}$Sr are measured at neutron energies of 19.44 ± 1.02 MeV and 16.81 ± 0.85 MeV to provide a data set at the above mentioned energies. The measurements and analysis of the data were done using standard neutron activation analysis and offline gamma-ray spectroscopy and then compared to EXFOR database. The method of tailing correction is used to remove the contribution of the low energy neutrons from the primary neutrons, which is adapted from literature (Smithet al., 2005; RajnikantMukherjee et al., 2017).

The aforementioned sections II and III provide in-depth information about the experimental details and data analysis respectively. The suitable corrections in neutron flux and average neutron energy employed to obtain accurate reaction cross-section are also discussed in section III. Section IV describes the theoretical calculations followed by results and discussion in section V. In Section VI conclusion is given.

## 2. Experimental details

The neutrons required to carry out this experiment were obtained from $^{7}$Li (p,n)$^{7}$Be reaction at the BARC-TIFR Pelletron facility in Mumbai, India. A natural lithium foil of thickness 3.4 mg/cm$^2$ was wrapped with a Tantalum foil of 3.7 mg/cm$^2$ in the front, then

* Corresponding author.
** Corresponding author.
*E-mail addresses:* nidhi08shetty@gmail.com (N. Shetty), r.j.makwana-phy@msubaroda.ac.in (R. Makwana).

https://doi.org/10.1016/j.apradiso.2019.108866
Received 23 March 2019; Received in revised form 20 July 2019; Accepted 14 August 2019
Available online 17 August 2019
0969-8043/ 

**Table 1**
Details of the irradiation experiment.

| | Irradiation 1 | Irradiation 2 |
|---|---|---|
| Proton Energy (MeV) | 22 | 19 |
| Total Irradiation Time (h:min) | 5:20 | 6:00 |
| Beam Current (nA) | 170 | 200 |

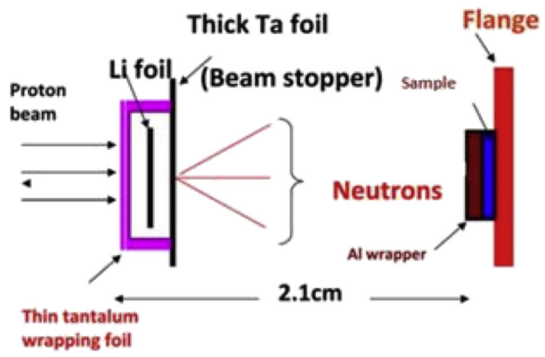


**Fig. 1.** Experimental arrangement for irradiation of neutrons from $^{7}$Li (p,n) reaction (Prajapati et al., 2012).

$2 \times 4.0\,mg/cm^2$ of Li and $4.12\,mg/cm^2$ in the back (Soni et al., 2018; RajnikantMukherjee et al., 2017). It was irradiated with a proton beam of energies 22.0 and 19.0 MeV. The distance between the Li foil and the sample was kept 2.1 cm in the forward direction. The different irradiation times for the target are given in Table 1. A schematic view of the irradiation setup is shown in Fig. 1. The Sr foils (natural form) with $10 \times 10 \times 0.3\,mm^3$ were used for the irradiation. The weight of the Sr foils was measured using a digital microbalance and were found to be 0.07971 g (Irradiation 1) and 0.0757 g for (Irradiation 2). To measure neutron flux, indium (In) was used as a flux monitor for both the irradiations. After irradiating the samples for the time duration mentioned in Table 1, they were cooled for a suitable time. Next, the samples were kept in front of a pre-calibrated high purity germanium detector by mounting them on a Perspex plate. A Baltic company HPGe detector with 4 k channels MCA and MAESTRO spectroscopic software was used to measure the γ-ray spectra from the irradiated sample. The detector was shielded with sufficient lead to stop the background radiation (specially 511 keV and 1.4 MeV). The calibration of HPGE detector and its efficiency at different gamma ray energies were determined using a standard $^{152}$Eu multi-gamma ray source. The activity of the samples was measured for various suitable counting times. The prominent gamma ray energies emitted from the sample and related spectroscopic data are given in Table 2. Isotopic abundances are taken from literature (http://www.nndc.bnl.gov/nudat2/index_dex.jsp). The threshold energies of the reactions are calculated using the Q value Calculator provided online by National Nuclear Data Center (NNDC) (http://www.nndc.bnl.gov/qcalc/index.jsp). Typical Gamma ray spectra from the irradiated Sr sample are shown in Fig. 2.

## 3. Data analysis

### 3.1. Neutron activation analysis

The standard neutron activation analysis technique was employed to analyze the experimental data. In this technique, nuclei are irradiated with neutrons, and activation is produced. The product nuclei, which formed from the irradiation, emit characteristic gamma rays having adequately long half life and gamma branching abundances, can be used for the activation measurement. Here, the number of target nuclei available and the neutron flux incident on the target determines the rate of production of product nuclei or the nuclear reaction rate. The cross-section of the selected reactions can be determined using the following equation (Rosman and P Taylor, 1998):

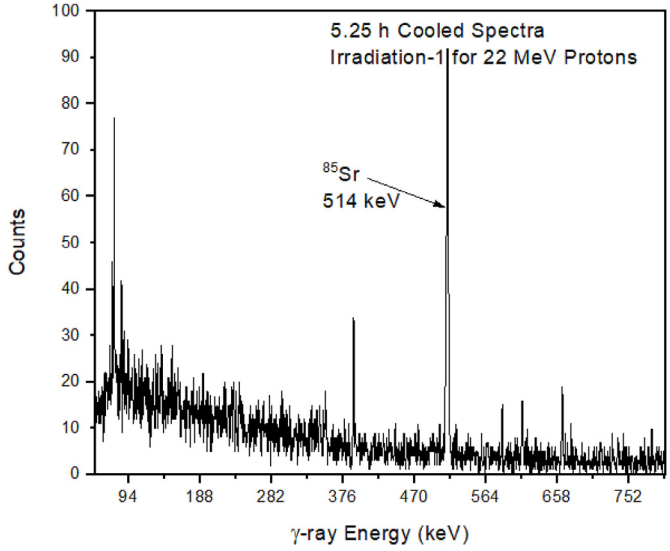


**Fig. 2.** Typical γ ray spectra from irradiated Sr target obtained using HPGe Detector.

$$\sigma = \frac{A_\gamma \lambda (T_{ct}/T_r)}{N\varphi I\gamma\varepsilon(1 - e^{-\lambda T_i})(1 - e^{-T_{ct}})e^{-\lambda T_{cl}}} \quad (1)$$

where.

$A_\gamma$ = number of detected γ-ray counts of the selected gamma energy;
λ = decay constant of the product nucleus ($s^{-1}$);
$T_i$ = Irradiation Time (s);
$T_{cl}$ = Cooling Time (s);
$T_{ct}$ = Counting Time (s);
φ = Incident neutron flux ($ncm^{-2}s^{-1}$);
$I_\gamma$ = branching intensity of γ-ray;
ε = efficiency of the detector for the chosen γ-ray;
N = Number of target atoms.

An HPGe detector was used to measure the activity Aγ for gamma ray of the selected energy. The experiment was performed to measure the cross section of the reaction $^{86}$Sr (n, 2n) $^{85}$Sr. In the present case the selected gamma ray energy is 514 keV emitted from $^{85}$Sr with branching intensity of 96%. A suitable γ-ray counting plan was devised based on the half-lives of the nuclei of interest and several rounds of counting were done. The dead time was below 4% during the entire process. The isotopic abundances and weight of the sample were used to calculate the number of target nuclei. A γ-ray spectrum of an irradiated indium (In) foil was used to calculate the neutron flux. Other standard parameters of the reaction were referred from the literature (http://

**Table 2**
Nuclear reaction and decay data in the present experiment.

| Reaction | Isotopic abundance (%) | Threshold Energy (MeV) | Product Nucleus | Half Life | Prominent γ-ray energy (keV); (branching intensity %) |
|---|---|---|---|---|---|
| **$^{86}$Sr(n, 2n)$^{85}$Sr** | 9.86 | 11.6 | $^{85}$Sr | 64.84 d | 514.0 (96) |

www.nndc.bnl.gov/nudat2/index_dex.jsp; http://www.nndc.bnl.gov/qcalc/index.jsp; Rosman and P Taylor, 1998; Vansola et al., 2015).

### 3.2. Neutron flux and average neutron energy

The $^{7}$Li (p,n)$^{7}$Be reaction was used to produce neutrons. This reaction acts as a mono-energetic neutron source of neutrons below 2.4 MeV proton energy (Vansola et al., 2015; Poppe et al., 1976). A second group of neutrons is produced above 2.4 MeV because the first excited state of $^{7}$Be gets populated. Apart from the main neutron group, three body interaction and other excited states also contribute in the neutron production in the energy range above 6 MeV (Vansola et al., 2015; Poppe et al., 1976).

The higher neutron flux and higher neutron energy (forming a peak) of the primary group of neutrons can be used to measure the cross-section. The cross-section is measured at this average peak energy, which can be calculated from the following:

$$E_{mean} = \frac{\int_{E_{ps}}^{E_{max}} E_i \varphi_i dE}{\int_{E_{ps}}^{E_{max}} \varphi_i dE} \quad (2)$$

where.

$E_{ps}$ = neutron energy from where the main peak starts,
$E_{max}$ = maximum neutron Energy;
$E_i$ = energy bin;
$\Phi_i$ = neutron flux of energy bin $E_i$;
$E_{mean}$ = Effective mean energy;

The neutron spectra for proton energy 22.0 and 19.0 MeV used in the calculations were derived from the data available in various literatures (Dyakonov et al., 1994; Poppe et al., 1976; Anderson et al., 1970; Prajapati et al., 2012; Mcnaughton et al., 1975; Lapenas, 1975). The derived neutron spectra used for the calculations are shown in Fig. 3 (A, B) and the average peak energies calculated by equation (2) are given in Table 3.

It is essential to accurately calculate the neutron flux in order to analyze the data. In this experiment, $^{115}$In(n,n')$^{115m}$In and $^{115}$In(n, 2n)$^{114m}$In were used as monitor reactions for the neutron flux measurement. The reaction product $^{115m}$In and $^{114m}$In has half-lives of 4.48 h and 49.51d respectively. We got poor statistics for $^{115}$In (n, 2n)$^{114m}$In reaction at 22 MeV which may lead to uncertainty in flux calculation. Hence we did not rely on it for neutron flux measurement at 22 MeV. A γ-ray spectrum of $^{115m}$In is shown in Fig. 4. The characteristic γ lines are shown in Table 4.

The neutron flux incident on the target was calculated using the spectrum-averaged cross-section for the monitor reaction. The relatively new data for $^{115}$In(n,n')$^{115m}$In from the EXFOR and IRDFF library (Lovestam et al., 2007; Agus et al., 2004; Uddin et al., 2013; Schherbakov et al., 2001; Shibata et al., 2011; Rochman et al., 2016) was used. The spectrum averaged cross-section was calculated using the following equation where:

$$\sigma_{av} = \frac{\int_{E_t}^{E_{max}} \sigma_i \varphi_i dE}{\int_{E_t}^{E_{max}} \varphi_i dE} \quad (3)$$

where.

$E_t$ = threshold energy of the monitor reaction;
$E_{max}$ = maximum neutron energy;
$\sigma_i$ = cross-section at energy $E_i$ for monitor reaction from EXFOR (Lovestam et al., 2007; Agus et al., 2004; Uddin et al., 2013; Schherbakov et al., 2001).
$\sigma_{av}$ = spectrum average cross-section.

Table 3 gives spectrum-averaged cross-section for the monitor reaction. The neutron flux incident on the target was determined by the following activation equation.

$$\varphi = \frac{A_\gamma \lambda (T_{ct}/T_r)}{N\sigma_{av} I\gamma\varepsilon (1 - e^{-\lambda T_i})(1 - e^{-T_{ct}})e^{-\lambda T_{cl}}} \quad (4)$$

All the parameters are same as mentioned in equation (1).

In the average cross-section calculations, the measured value of neutron flux from the monitor was used as they were within the limits of experimental errors as discussed in section V.

### 3.3. Cross-section correction for low energy neutrons

In order to accurately measure the cross-section, it is necessary to make corrections due to the contribution from the lower energy neutrons (EXFOR). This correction is not needed if the source is mono-energetic unlike the present case. The neutron spectra used in this experiment includes various neutrons groups like the one arising due to the excited state of $^{7}$Be and three body interactions above 2.4 and 6 MeV respectively along with the primary neutron group as mentioned earlier (RajnikantMukherjee et al., 2017; Vansola et al., 2015; Poppe et al., 1976). Neutrons are produced by these secondary groups have lower energies along with the primary neutrons (RajnikantMukherjee

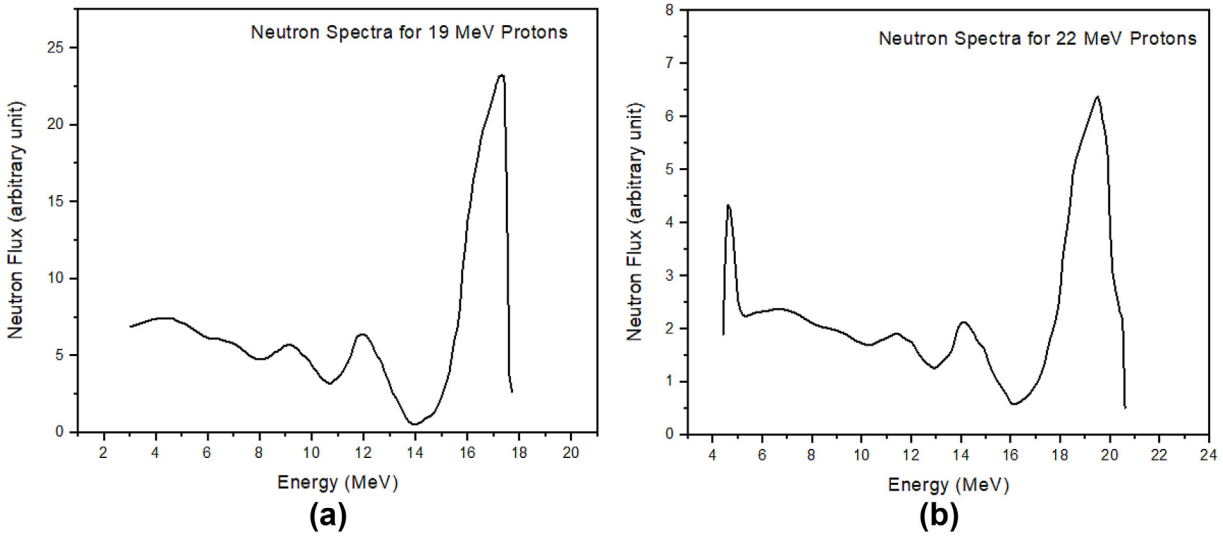


**Fig. 3.** (A) $^{7}$Li (p, n)$^{7}$Be spectra for 19 MeV proton energy. (B) $^{7}$Li (p,n)$^{7}$Be spectra for 22 MeV proton energy.

**Table 3**
The spectrum averaged neutron energies and respective spectrum averaged cross section, and measured neutron flux from monitor reaction.

| | Irradiation 1 | Irradiation 2 |
|---|---|---|
| Proton Energy (MeV) | 22 | 19 |
| Neutron Energy [from eqn-2] (MeV) | 19.44 ± 1.02 | 16.81 ± 0.85 |
| Spectrum averaged cross-section for In monitor (barns) using EXFOR | 0.15046 | 0.19498 |
| Calculated neutron flux from $^{115}$In(n,n')$^{115m}$In (ncm$^{-2}$s$^{-1}$) using EXFOR | $2.78 \times 10^7$ | $2.21 \times 10^7$ |
| Spectrum averaged cross-section for In monitor (barns) using IRDFF | 0.17165 | 0.19077 |
| Calculated neutron flux from $^{115}$In(n,n')$^{115m}$In (ncm$^{-2}$s$^{-1}$) using IRDFF | $2.55 \times 10^7$ | $2.84 \times 10^7$ |
| Calculated neutron flux from $^{115}$In(n, 2n)$^{114m}$In (ncm$^{-2}$s$^{-1}$) using IRDFF | – | $2.59 \times 10^7$ |

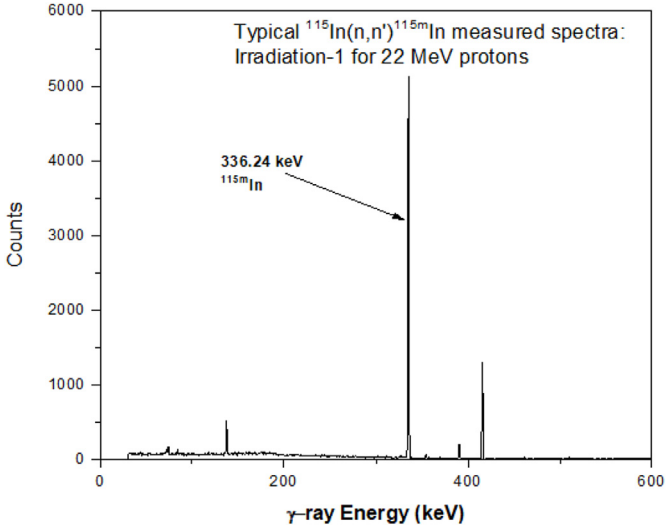


**Fig. 4.** Typical γ ray spectra from irradiated $^{115}$In using HPGe detector.

**Table 4**
Details of the monitor reactions with the product nucleus and prominent γ lines.

| Monitor Reaction | Product nucleus (half-life) (RajnikantMukherjee et al., 2017) | Prominent γ line |
|---|---|---|
| **$^{115}$In(n,n')$^{115m}$In** | $^{115m}$In(4.486 h) | 336.24 (45.8) |
| **$^{115}$In(n, 2n)$^{114m}$In** | $^{114m}$In (49.51 d) | 192.92 (15.56) |

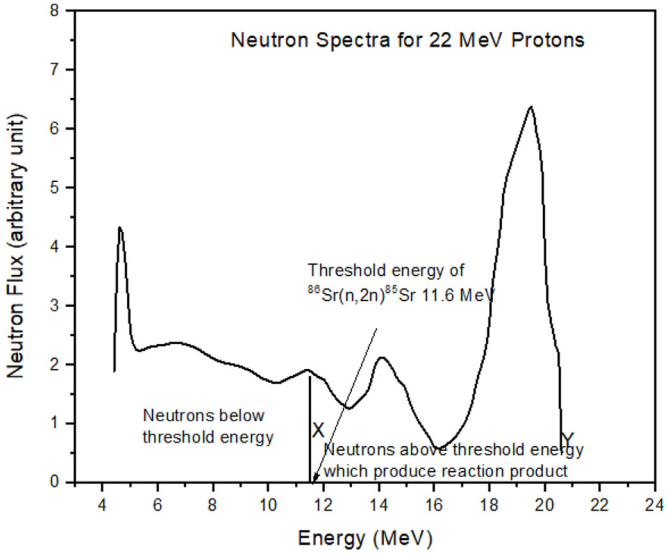


**Fig. 5.** Neutron Flux correction for threshold energy reactions shown for $^{86}$Sr (n, 2n)$^{85}$Sr reaction having a threshold energy of 11.6 MeV.

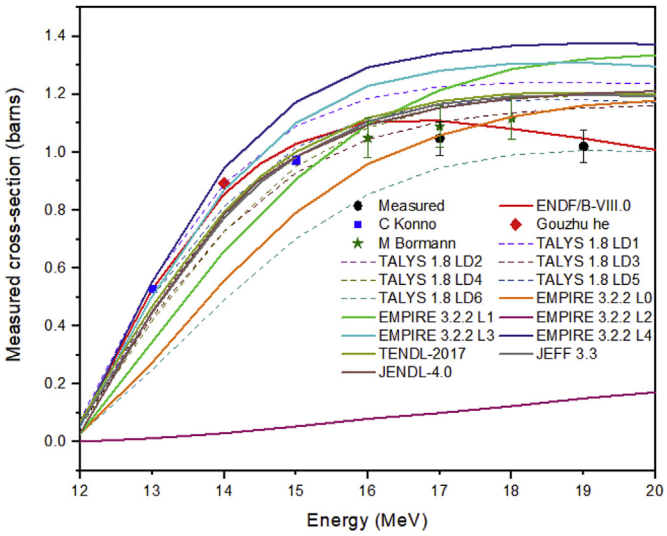


**Fig. 6.** Present measured cross-section for $^{86}$Sr (n, 2n)$^{85}$Sr reaction compared with EXFOR data, ENDF/B-VIII.0, and predicted cross-section data using different LD models using nuclear modular codes of TALYS 1.8 (LD1 to LD6) and EMPIRE 3.2.2 (L0 to L4).

et al., 2017; Vansola et al., 2015; Poppe et al., 1976). The primary neutrons can be considered as a quasi-monoenergetic source because it exhibits a distant broad peak at a much higher energy and a greater flux. A process called tailing correction makes it possible to remove the contribution of the low energy neutron from the primary neutrons. The method of tailing correction used has been adapted from the literature (Smithet al., 2005). Following steps have been followed in order to do corrections.

1. The neutron flux measured and calculated from monitor reactions and Neutron Activation Analysis (eq (1)) were used to calculate the reaction cross-section. For the reactions having threshold energy, a correction in the neutron flux must be done whereas total neutron flux can be used for no threshold energy reaction (e.g. capture reaction) (RajnikantMukherjee et al., 2017). The correction can be made by taking the partial neutron flux from the area under the neutron spectra from minimum to threshold energy neutrons and subtracting it from the measured neutron flux. The $^{86}$Sr (n, 2n)$^{85}$Sr has a threshold energy of 11.6 MeV. Thus, the flux for this reaction should be the area under the curve from 'X' (threshold energy) to 'Y' (max. neutron energy) shown in Fig. 5. This way, the actual neutron flux used to produce product isotope can be corrected. This neutron flux has been used to calculate the measured the cross-section.
2. The reaction cross-section at different neutron energy were obtained from theoretical calculations using nuclear modular code TALYS 1.8 and have been used to remove effective spectrum average cross-section from the threshold to the minimum energy of the peak of interest ($E_{ps}$). These calculated cross-section at different energies are convoluted with neutron flux given in Fig. 3 (A, B)

**Table 5**
Comparison of the present experimental data with different model predictions using TALYS 1.8 and EMPIRE 3.2.2

| Neutron Energy (MeV) | Measured Cross-section (barns) | TALYS1.8 | | | | | EMPIRE 3.2.2 | | | | | |
|---|---|---|---|---|---|---|---|---|---|---|---|---|
| | | LD1 | LD2 | LD3 | LD4 | LD5 | LD6 | L0 | L1 | L2 | L3 | L4 |
| 19.44 ± 1.02 | 1.0715 ± 0.06 | 1.2411 | 1.2076 | 1.1533 | 1.1966 | 1.1808 | 1.0062 | 1.16192 | 1.32151 | 0.150699 | 1.30987 | 1.37661 |
| 16.81 ± 0.85 | 1.0456 ± 0.05 | 1.2266 | 1.1772 | 1.1056 | 1.1534 | 1.1641 | 0.9470 | 1.0587 | 1.21472 | 0.100254 | 1.28198 | 1.34217 |

(RajnikantMukherjee et al., 2017). The spectrum average cross-section calculated from threshold to minimum energy ($E_{ps}$) was subtracted from the previous calculated cross-section data set. By this correction, one can obtain reaction cross-section at the spectrum averaged neutron peak energy.

3. The cross-section for $^{86}$Sr (n, 2n)$^{85}$Sr has been measured at neutron energies 19.44 ± 1.02 and 16.81 ± 0.85 MeV. The 514 keV gamma ray with intensity 0.96 is common to both $^{84}$Sr (n,γ) and $^{86}$Sr (n, 2n). Thus, it is important to remove the part of cross-section from the capture reaction. Compared to the lower energy neutrons, the (n,γ) reaction contributes significantly less at higher energy neutrons. Further the spectrum averaged cross section for $^{84}$Sr (n,γ) was calculated and subtracted from the measured cross section. Hence, the cross-section obtained is purely due to the (n, 2n) reaction. This will give final cross section of the reaction at peak average neutron energy for $^{86}$Sr (n, 2n) reaction.

## 4. Theoretical calculations

Two nuclear reaction modular codes namely: TALYS 1.8 and EMPIRE 3.2.2 have been used to theoretically understand the measured cross-section results. Both these codes are used worldwide to accurately predict the nuclear data for the emission of γ, neutron, proton, deuteron, Triton and other particles. Both codes use reaction parameters from the RIPL database (Capote et al., 2009). The effects of compound, pre-equilibrium, level density parameters and direct reaction mechanism as a function of incident particle energy have been considered in these codes. The Hauscher–Feschbach model was used to incorporate the compound reaction mechanism, and the global potential-proposed by Koning ad Delaroche was used to obtain optical model parameters (Hauser and Feshbach, 1952; Kalbach, 1986). The Exciton model developed by Kalbach was used to account for the pre-equilibrium contribution (Gilbert and Cameron, 1965). The present calculations were done using all the default parameters. Only the LD model and Level Density parameters have been changed. The results have been compared with EXFOR and ENDF/B-VIII.0 data and have been shown in Fig. 6.

As it can be seen from the graph, apart from ENDF/B-VIII.0, L0 and L1 models of EMPIRE 3.2.2 give a relatively better agreement with the present experimental results. For TALYS 1.8, except for LD1 and LD6, all the LD models are well in agreement with the experimental data.

## 5. Results and discussion

The present study was carried out to provide a nuclear reaction cross-section data set in the energy range where there is a scarcity of data. The measured values of the cross section at neutron energies 19.44 ± 1.02 and 16.81 ± 0.85 MeV are 1.0715 ± 0.06 b and 1.0456 ± 0.05 b respectively. The measured data has been compared to the evaluated data using TALYS 1.8 and EMPIRE 3.2.2 (Koning et al., 2013; Herman et al., 2007). The different LD models of TALYS 1.8 i.e. LD model 1 to LD model 6 was used to evaluate the theoretical cross-section for the selected nuclear reaction and was compared with the experimental data. The resuts are shown in Table 5. The details about these parameters are available in TALYS 1.8 manual (Koning et al., 2013; Herman et al., 2007; https://www-nds.iaea.org/RIPL-3/densities/). EMPIRE 3.2.2 also provides different options for level density. The level density parameter values levden = 0, 1, 2, 3, 4 uses various well-known models described in various publications. (Prajapati et al., 2012; Ignatyuk et al., 1979, 1993; Hilaire et al., 2012; Capote et al., 2012). The cross-sections from threshold energy to 20 MeV were calculated by varying these parameters. The predicted and experimental results are shown in Fig. 6.

## 6. Conclusion

Cross-Sections $^{86}$Sr (n, 2n)$^{85}$Sr reactions were measured at neutron energies 19.44 ± 1.02 and 16.81 ± 0.85 MeV by employing Neutron Activation Analysis technique and incorporating standard tailing corrections. These cross-sections fall in the energy range where there are very few measured data with scarcity. Various correction terms were used in the present work along with the spectrum averaged neutron energy and accurate flux measurements. Indium has been used as a flux monitor. The cross-section measurements have been compared with ENDF/B-VIII.0, theoretical nuclear codes TALYS 1.8 and EMPIRE 3.2.2. It can be concluded that the measured data is well in agreement with ENDF/B-VIII.0. It is also observed that all the EXFOR data agree with ENDF/B-VIII.0 data. All the other prediction are showing discrepancies with the experimental data. The cross-section data presented in this work are important for the future fission/fusion reactor technology. As the Sr-90 is used in a super conductor, it is necessary to produce more data which can show its capability to remain super conductor under high energy radiation zone.

## Acknowledgement

The author (RJM) acknowledge UGC-DAE Consortium for Scientific Research, Kolkata Centre for providing a research project: UGC.DAE-CSR-KC/CRS/19NPO8/0919 to carry out research work.

## Appendix A. Supplementary data

Supplementary data to this article can be found online at https://doi.org/10.1016/j.apradiso.2019.108866.

## References

Agus, Y., Celenk, I., Ozmen, A., 2004. Measurement of cross sections of threshold detectorswith spectrum average technique. Radiochim. Acta 92, 63.
Anderson, J.D., Wong, C., Madsen, V.A., 1970. Charge exchange part of the effective twobodyinteraction. Phys. Rev. Lett. 24, 1074.
Capote, R., Herman, M., Oblo zinsky, P., Young, P.G., Goriely, S., Belgya, T., Ignatyuk, A.V., Koning, A.J., Hilaire, S., Plujko, V.A., Avrigeanu, M., Bersillon, O., Chadwick, M.B., Fukahori, T., Zhigang, Ge, Han, Y., Kailas, S., Kopecky, J., Maslov, V.M., Reffo, G., Sin, M., Soukhovitskii, E.Sh, Talou, P., 2009. RIPL – reference input parameter library for calculation of nuclear reactions and nuclear data evaluations. Nucl. Data Sheets 110, 3107–3214 A. J. Koning and J. P. Declaroche, Nucl. Phys. A 713, 231 (2003).
Capote, R., Zolotarev, K.I., Pronyaev, V.G., Trkov, A., April 2012. J. ASTM Int. (JAI) 9 (Issue 4) JAI104119.
Dyakonov, V.P., Markovich, V.I., Puzniak, R., Szymczak, H., Doroshenko, N.A., Yuzhelevskii, Ya I., 1994. Influence of strontium on superconducting and magnetic properties of $DyBa_{2-x}Sr_xCu_3O_{7-\delta}$. Phys. C Supercond. 225, 51.
EXFOR Experimental nuclear reaction data. https://www-nds.iaea.org/exfor/.
Gilbert, A., Cameron, A.G.W., 1965. A composite nuclear-level density formula with shell corrections. Can. J. Phys. 43 (8), 1446–1496.
Hauser, W., Feshbach, H., 1952. The inelastic scattering of neutrons. Phys. Rev. 87, 366.

Herman, M., Capote, R., Carlson, B.V., Oblozinsky, P., Sin, M., Trkov, A., Wienke, H., Zerkin, V., 2007. EMPIRE: nuclear reaction model code system for data evaluation. Nucl. Data Sheets 108, 2655–2715.

Hilaire, S., Girod, M., Goriely, S., Koning, A.J., 2012. Temperature dependent combinatorial level densities with the D1M Gogny force. Phys. Rev. C 86, 064317.

Ignatyuk, A.V., Istekov, K.K., Smirenkin, G.N., 1979. The role of collective effects in the systematics of nuclear level densities. Sov. J. Nucl. Phys. 29, 450.

Ignatyuk, A.V., Weil, J.L., Raman, S., Kahane, S., 1993. Density of discrete levels in $^{116}$Sn. Phys. Rev. C 47, 1504.

Kalbach, C., 1986. Two-component exciton model: basic formalism away from shell closures. Phys. Rev. C 33, 818.

Koning, A.J., Blomgren, J., 2009. Nuclear Data for Sustainable Nuclear Energy, JRC Scientific and Technical Report No. EUR23977EN-2009. retrieved from. https://cordis.europa.eu/pub/fp6-euratom/docsc/candide-final-report_en.pdf.

Koning, A., Hilaire, S., Goriely, S., 2013. first ed. TALYS-1.6- A Nuclear Reaction Programme, User Manual NRG, Westerduinweg.

Lapenas, A.A., 1975. Izmerenie Spektrov Nejtronov Aktivacionym Metodom" PublishingHouse "ZINATNE. Riga, USSR (1975), (It contains an evaluation of 22 dosimetryreactions).

Lovestam, G., Hult, M., Fessler, A., Gamboni, T., Gasparro, J., Jaime, R., 2007. Measurement of neutron excitation functions using wide energy neutron beams. Nucl. Instrum. Methods Phys. Res., Sect. A 580, 1400.

M.W. Mcnaughton, N. S. P. King, F. P. Brady, J. L. Romero, and, T. S. Subramanian, Measurements of $^{7}$Li(p,n) and $^{9}$Be(p, n) cross sections at 15, 20 and 30 MeV, 1975. Nucl. Instrum. Methods 130, 555.

Poppe, C.H., Anderson, J.D., Davis, J.C., Grimes, S.M., Wong, C., 1976. Cross section for the $^{7}$Li(p, n)$^{7}$Be reaction between 4.2 and 26 MeV. Phys. Rev. C 14, 438.

Prajapati, P.M., Naik, H., Suryanarayana, S.V., Mukherjee Jagadeesan, S., Sharma, K.C., Thakre, S.C., Rasheed, S.V., Ganesan, K.K., Goswami, A.,S., 2012. Measurement of the neutron capture cross-sections of $^{232}$Th at 5.9 MeV and 15.5 MeV. Eur. Phys. J. A48, 35.

Rajnikant, Makwana, Mukherjee, S., Mishra, P., Naik, H., Singh, N.L., Mehta, M., Katovsky, K., Suryanarayana, S.V., Vansola, V., Santhi Sheela, Y., Karkera, M., Acharya, A., Khirwadkar, S., 2017. Measurement of the cross section of the $^{186}$ W(n, γ)$^{187}$ W, $^{182}$ W(n, $^{182}$ Ta, $^{154}$ Gd(n, 2n)$^{153}$Gd, and $^{160}$Gd(n, 2n)$^{159}$Gd reaction at neutron energies of 5 to 17 MeV. Phys. Rev. C 96, 02408.

Retrieved from: http://www.nndc.bnl.gov/nudat2/index_dex.jsp.

Retrieved from: http://www.nndc.bnl.gov/qcalc/index.jsp.

Retrieved from: https://www-nds.iaea.org/RIPL-3/densities/.

Rochman, D., Koning, A.J., Sublet, J.Ch, Fleming, M., et al., 2016. The TENDL library: hope, reality and future. In: Proceedings of the International Conference on Nuclear Data for Science and Technology, September 11-16, (Bruges, Belgium).

Rosman, K.J.R., P Taylor, P.D., 1998. Isotopic compositions of the elements. Pure Appl. Chem. 70, 217.

Schherbakov, O.A., Donets, A. Yu, Evdokimov, A.V., et al., 2001. International Seminar on Interactions of Neutrons with Nuclei, Dubna, Russia, vol 9. pp. 257.

Shibata, K., Iwamoto, O., Nakagawa, T., Iwamoto, N., Ichihara, A., Kunieda, S., Chiba, S., Furutaka, K., Otuka, N., Ohsawa, T., Murata, T., Matsunobu, H., Zukeran, A., Kamada, S., Katakura, J., 2011. JENDL-4.0: a new library for nuclear science and engineering. J. Nucl. Sci. Technol. 48 (1), 1–30.

Smith, D.L.et al., Corrections for low energy neutrons by spectral indexing. retrieved from: https://www.oecdnea.org/science/docs/2005/nsc-wpec-doc2005-357.pdf.

Soni, B.K., Makwana, Rajnikant, Mukherjee, S., Parashari, Siddharth, Suryanarayana, S.V., Nayak, B.K., Naik, H., Mehta, M., 2018. Neutron capture cross-sections for $^{159}$Tb isotope in the energy range of 5 to17 MeV. Appl. Radiat. Isot. 141, 10.

Uddin, M.S., Sudar, S., Hossain, S.M., Khan, R., Zulquarnain, M.A., Qaim, S.M., 2013. Fast neutron spectrum unfolding of a TRIGA Mark II reactor and measurement of spectrum-averaged cross sections: integral tests of differential cross sections of neutron threshold reactions. Radiochim. Acta 101, 613.

Vansola, Vibha, Ghosh, Reetuparna, Badwar, Sylvia, Mary Lawriniang, Bioletty, Gopalakrishna, Arjun, Naik, Haladhara, Naik, Yeshwant, Subhash Tawade, Nilesh, Sharma, Suresh Chand, Pravinchandra Bhatt, Jignesh, Gupta, Shri Krishna, Sarode, Shankar, Mukherjee, Surjit, Singh, Nand Lal, Singh, Pitambar, Goswami, Ashok, 2015. Measurement of$^{197}$Au(n,γ)$^{198g}$Au reaction cross-section at the neutron energies of 1.12,2.12, 3.12 and 4.12MeV. Radiochem. Acta 103, 817.

Zsolnay, E.M., Capote, R., Nolthenius, H.K., Trkov, A., 2012. Technical Report INDC(NDS)-0616. IAEA, Vienna.